Journal of Zhejiang University SCIENCE A
ISSN 1673-565X (Print); ISSN 1862-1775 (Online)
www.zju.edu.cn/jzus; www.springerlink.com
E-mail: jzus@zju.edu.cn

Analysis of a new 5-phase bearingless induction motor*

HUANG Jin, KANG Min, YANG Jia-qiang†‡

(*School of Electrical Engineering, Zhejiang University, Hangzhou 310027, China*)

†E-mail: yjq1998@163.com

Received Mar. 2, 2007; revision accepted Apr. 2, 2007

Abstract: This paper addresses the bearingless motor with a single set of multiphase windings. The interaction between M and $M\pm1$ pole-pair magnetic fields produces radial force. Based on this principle, a bearingless machine is obtained. Conventional bearingless machine has dual windings, levitation windings and torque windings, which produce the two magnetic fields. In the proposed bearingless motor, the two needed magnetic fields are produced by feeding two groups of currents to a single set of multiphase windings. Taking a 5-phase induction motor as example, the inductance matrices, considering air gap eccentricity, are calculated with the modified winding function method. The radial force analytical model is deduced by virtual displacement, and its results are validated by FEA. The mathematical model of the new bearingless machine is set up, and the simulation results verified the feasibility of this novel bearingless motor.

Key words: Air-gap-flux-oriented control, Bearingless motor, Multiphase, Radial force, Single set of windings, Modified winding function method

doi:10.1631/jzus.2007.A1311 **Document code:** A **CLC number:** TM301; TM303

INTRODUCTION

A bearingless motor is an integrated device that can produce rotor levitation force as well as torque (Chiba *et al*., 1994). The winding configurations of bearingless motors can be categorized into two groups: dual set of winding configurations and single set of winding configurations. Most bearingless motors belong to the former category. Its stator is composed of two separate sets of windings, and the difference of their pole-pair numbers is 1. The primary winding carries the "motor currents" which drive the motor, while the secondary winding carries the "levitation currents" which suspend the rotor.

Bearingless motors with bridge configured windings (Khoo, 2005) and with divided windings (Ferreira *et al*., 2005) belong to the latter category. They produce radial force by intentionally unbalancing the magnetic fields. The bearingless motor with a single set of windings possesses advantages such as: (1) simpler construction, requiring only one set of windings; (2) relatively low power loss (Khoo, 2005).

A multiphase motor (phase number $n\geq5$) has multiple orthogonal d-q planes. One d-q plane can be used for torque control, and the additional degrees of freedom can be used in a different manner. Xu *et al*.(2001) used the additional degrees of freedom to enhance the torque production through injection of higher order current harmonics, while Levi *et al.*(2004) utilized the additional degrees of freedom to control independently other machines within a multiphase multi-motor system. Osama and Lipo (1997; 1999) utilized the additional degrees of freedom of a 6-phase induction motor to realize pole changing and bearing relief. This paper presents a bearingless motor with multiphase windings, which produces the two needed magnetic fields by feeding two groups of currents to the single set of multiphase windings with a multiphase converter. In other words, one d-q plane is used for motor drive, and the other d-q plane is used for rotor levitation. The proposed motor has many advantages over conventional bearingless motors.

‡ Corresponding author

* Project (No. 50677060) supported by the National Natural Science Foundation of China

PRINCIPLE OF BEARINGLESS MOTOR WITH SINGLE SET OF MULTIPHASE WINDINGS

Principles of radial force generation of multiphase motor

The rotor of a bearingless motor is levitated by radial force. The interaction between M and $M\pm1$ pole-pair magnetic fields in the air gap generates radial forces, which are used to levitate the rotor (Okada *et al*., 1995). Conventional bearingless motors produce levitation force by two sets of 3-phase windings, and the difference of their pole-pair numbers is 1 (Chiba *et al*., 1994). A bearingless motor with a single set of multiphase windings is presented.

Windings in a motor are usually represented with winding function (Luo *et al*., 1995; Osama and Lipo, 1997). The winding function of winding "a" represents the MMF distribution along the air gap for a unit current flowing in winding "a". In an n-phase symmetric system, the winding functions of each phase can be written as Fourier series:

$$\begin{cases} N_a = N_1\cos\theta + N_2\cos(2\theta) + N_3\cos(3\theta) + \cdots, \\ N_b = N_1\cos(\theta-\xi) + N_2\cos[2(\theta-\xi)] \\ \quad + N_3\cos[3(\theta-\xi)] + \cdots, \\ N_c = N_1\cos(\theta-2\xi) + N_2\cos[2(\theta-2\xi)] \\ \quad + N_3\cos[3(\theta-2\xi)] + \cdots, \\ \quad \cdots \\ N_n = N_1\cos[\theta-(n-1)\xi] + N_2\cos\{2[\theta- \\ \quad (n-1)\xi]\} + N_3\cos\{3[\theta-(n-1)\xi]\} + \cdots, \end{cases} \tag{1}$$

where $\xi=2\pi/n$, θ is the angular position along the stator inner surface, and N_1, N_2, N_3 are coefficients of winding function.

To be convenient for expression, the group of currents below is defined as "n phase k pole-pair currents $\boldsymbol{I}_k$":

$$\begin{cases} I_a = I_{km}\cos(\omega t + \Phi_k), \\ I_b = I_{km}\cos(\omega t + \Phi_k - k\xi), \\ I_c = I_{km}\cos(\omega t + \Phi_k - 2k\xi), \\ \quad \cdots \\ I_n = I_{km}\cos[\omega t + \Phi_k - (n-1)k\xi], \end{cases} \tag{2}$$

where I_{km} is the amplitude of $\boldsymbol{I}_k$ (k=1,2,3,…) and Φ_k is the phase angle at t=0 of I_a. The MMF wave of an n-phase symmetric system fed by $\boldsymbol{I}_k$ can be expressed as

$$\begin{aligned} F &= \sum_{i=1}^{n}\{I_{km}\cos[\omega t + \Phi_k - k(i-1)\xi] \\ &\quad \cdot \sum_{\nu} N_\nu \cos\{\nu[\theta-(i-1)\xi]\}\} \\ &= \frac{I_{km}}{2}\sum_{i=1}^{n}\sum_{\nu} N_\nu\{\cos[\omega t + \Phi_k + \nu\theta - (k+\nu)(i-1)\xi] \\ &\quad + \cos[\omega t + \Phi_k - \nu\theta - (k-\nu)(i-1)\xi]\}. \end{aligned} \tag{3}$$

So the νth harmonic MMF wave is

$$F_\nu = \begin{cases} nN_\nu I_{km}\cos(\omega t + \Phi_k + \nu\theta)/2, & k+\nu = \mu n, \\ 0, & k\pm\nu \neq \mu n, \\ nN_\nu I_{km}\cos(\omega t + \Phi_k - \nu\theta)/2, & k-\nu = \mu n, \end{cases} \tag{4}$$

where $\mu\in\mathbb{Z}$.

It is suggested that in an n-phase winding motor ($n\geq5$), "n phase 1 pole-pair current" $\boldsymbol{I}_1$ generates 1 pole-pair revolving magnetic field in the air gap, and $\boldsymbol{I}_2$ generates 2 pole-pair revolving magnetic field. So a bearingless motor with multiphase windings can be realized by properly controlling $\boldsymbol{I}_1$ and $\boldsymbol{I}_2$.

Stator configuration of a bearingless motor with multiphase windings

A 5-phase winding configuration is shown in Fig.1. The conductors of phase **a** go into slots "A" and return via slots "a". The 5-phase windings are identical and each of them is 72° displaced in angular space around the stator.

From Eq.(4), however, in the 5-phase motor, $\boldsymbol{I}_2$ generates F_2 and F_3. The interaction between them also generates radial force, which interferes with the levitation force generated by F_1 and F_2. A solution to this problem is to adjust the coil pitch to make N_3=0,

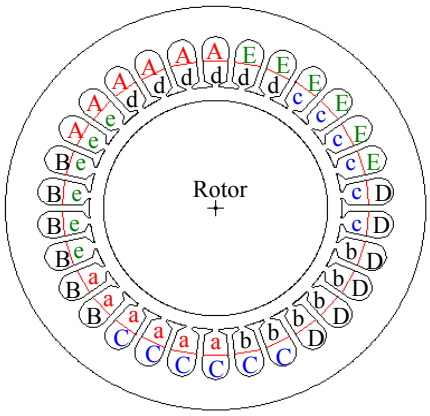

Fig.1 5-phase winding configuration of a bearingless motor (30 slots)

because F_3 is directly proportional to N_3. The coefficients N_ν with respect to coil pitch, calculated by FFT, are shown in Fig.2. Therefore, the coils span 10 slots in the bearingless motor as shown in Fig.1.

Fig.3 shows the flux distribution in the 5-phase motor shown in Fig.1. $\boldsymbol{I}_1$ generates 1 pole-pair magnetic field in the air gap, and $\boldsymbol{I}_2$ generates 2 pole-pair magnetic field. The two magnetic fields are generated simultaneously when the motor is fed by $\boldsymbol{I}_1+\boldsymbol{I}_2$, and then radial force is produced. Similar results can be obtained in other n-phase motors (n>5) if the coils are properly arranged.

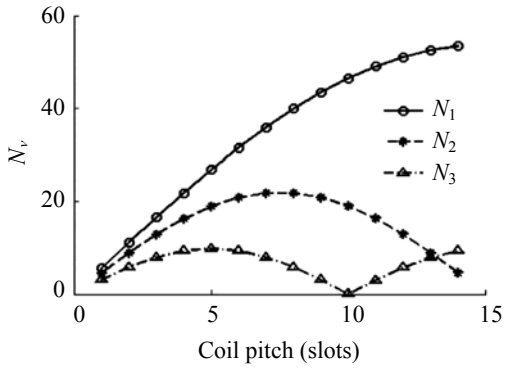

Fig.2 Coefficients N_ν vs coil pitch (15 turns per coil)

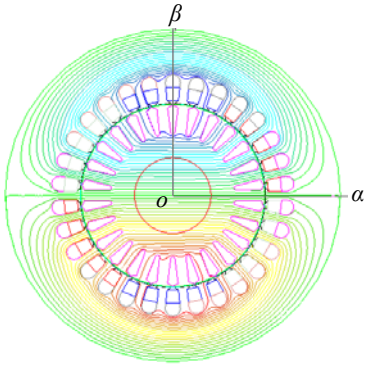

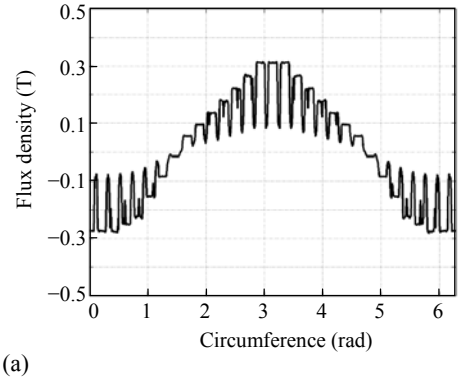

(a)

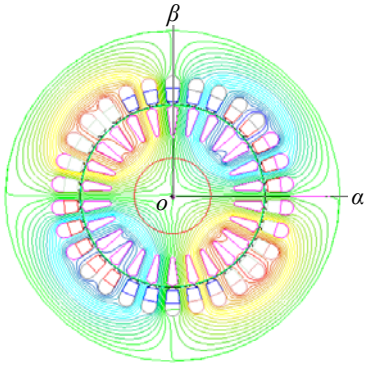

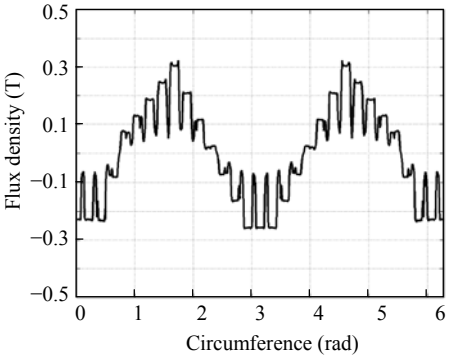

(b)

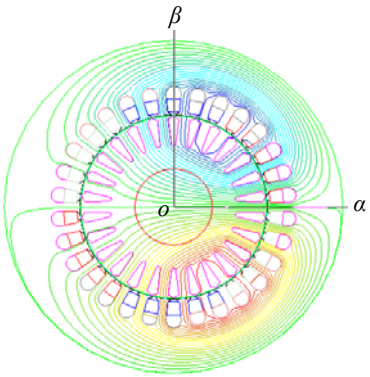

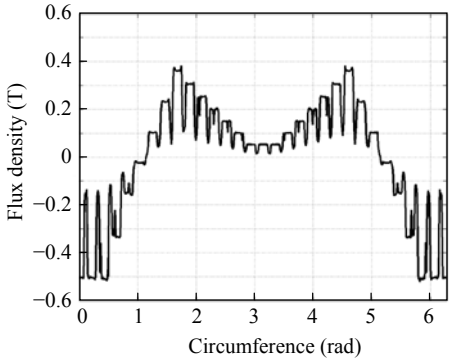

(c)

Fig.3 Flux and flux density on circumference when the motor is fed. (a) "5-phase 1-pole-pair currents" $\boldsymbol{I}_1$ ($\boldsymbol{I}_{1m}$=1 A, $\boldsymbol{\Phi}_1$=0); (b) "5-phase 2-pole-pair currents" $\boldsymbol{I}_2$ ($\boldsymbol{I}_{2m}$=2 A, $\boldsymbol{\Phi}_2$=0); (c) $\boldsymbol{I}_1+\boldsymbol{I}_2$

MATHEMATICAL MODEL OF BEARINGLESS MOTOR WITH MULTIPHASE WINDINGS

Calculation of inductance matrices in synchronously rotating reference frame

A bearingless motor works when it has a non-uniform air gap. Its inductances under eccentricity can be calculated with modified winding function method. The mutual inductance between winding "*a*" and "*b*" is (Faiz and Tabatabaei, 2002):

$$L_{ab}=2\pi u_0 lr<Pn_a n_b>-2\pi u_0 lr<Pn_a><Pn_b>/<P>, \quad (5)$$

where n_a and n_b are the turn functions of winding "*a*" and "*b*" respectively (Faiz and Tabatabaei, 2002), $P(\theta)$ is the distribution of inverse of air gap, g_0 is the radial length of a uniform air gap (as shown in Fig.4), and μ_0 is the air permeability. Operator $<f>$ is defined as the mean of function f over $[0, 2\pi]$. N_a and N_b are winding functions of winding "*a*" and "*b*", respectively.

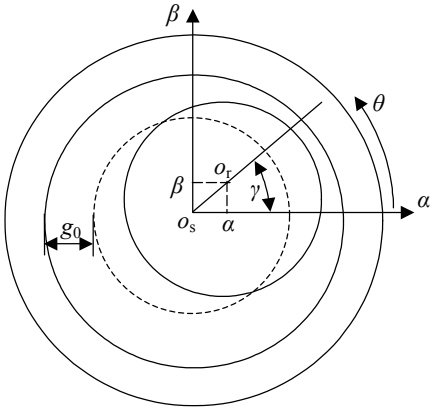

Fig.4 Air-gap eccentricity

It is obvious that $N_a=n_a-<n_a>$, so Eq.(5) can be rewritten as

$$L_{ab}=2\pi u_0 lr<PN_a N_b>-2\pi u_0 lr<PN_a><PN_b>/<P>. \quad (6)$$

The distribution of inverse of air gap can be described as

$$\begin{aligned} P(\theta) &= 1/\{g_0[1-\rho\cos(\theta-\gamma)]\} \\ &= (1/g_0)[(1+\rho^2/2)+\rho\cos(\theta-\gamma) \\ &+ \rho^2\cos^2(\theta-\gamma)/2+\rho^3\cos^3(\theta-\gamma)/4+\cdots], \end{aligned} \quad (7)$$

where $\rho=\sqrt{\alpha^2+\beta^2}/g_0$, α and β are the displacement of rotor center, as shown in Fig.4.

Matrix $\boldsymbol{C}_s$ [see Eq.(8) in P1315] is used to transform the voltages and currents of stator to synchronous reference frame (Huang, 1994; Levi *et al*., 2004). Where n is the phase number of stator or rotor. If n is odd, the last row in the matrix should be deleted. In the stator transformation matrix $\boldsymbol{C}_s$, $\varphi=\int\omega_1 dt$, ω_1 is the synchronous speed. Similarly, the rotor transformation matrix $\boldsymbol{C}_r$ can be obtained.

Taking a 5-phase induction motor for example, $\boldsymbol{L}_s$ is the stator inductance matrix, which can be transformed to the synchronously rotating reference frame:

$$\boldsymbol{L}_{st}=\boldsymbol{C}_s\boldsymbol{L}_s\boldsymbol{C}_s^{T}. \quad (9)$$

Omitting the zero sequence inductance, Eq.(9) can be rewritten as Eq.(10) (see P1315). Where $L_{1m}=3\pi\mu_0 lrN_1^2/g_0$, $L_{2m}=3\pi\mu_0 lrN_2^2/g_0$, L_{0s1} and L_{0s2} are leakage inductances of 1-pole-pair and 2-pole-pair equivalent windings respectively.

Similarly, the rotor inductance matrix and mutual inductance matrix between stator and rotor, under eccentricity in synchronously rotating reference frame, can be calculated as Eqs.(11) and (12) (see P1315). Where L_{0r1} and L_{0r2} are relevant rotor leakage inductances, and the rotor inductances are referred to the stator.

Voltage equations

In normal operating conditions, the rotor displacement is very small, and the equations under eccentricity are very complex, so the equations under no eccentricity are used to design the control system. Voltage equations in stationary reference frame are given by

$$\begin{bmatrix}\boldsymbol{U}_s\\ \boldsymbol{U}_r\end{bmatrix}=\begin{bmatrix}\boldsymbol{R}_s & \boldsymbol{0}\\ \boldsymbol{0} & \boldsymbol{R}_r\end{bmatrix}\begin{bmatrix}\boldsymbol{I}_s\\ \boldsymbol{I}_r\end{bmatrix}+p\begin{bmatrix}\boldsymbol{L}_s & \boldsymbol{M}_{sr}\\ \boldsymbol{M}_{sr}^{T} & \boldsymbol{L}_r\end{bmatrix}\begin{bmatrix}\boldsymbol{I}_s\\ \boldsymbol{I}_r\end{bmatrix}, \quad (13)$$

where $\boldsymbol{U}_s$ and $\boldsymbol{U}_r$ are voltage vectors of stator and rotor loops respectively (Luo *et al*., 1995), and p is the differential operator. By applying the transformation to the stator and rotor voltages and flux linkages, the voltage equations are rewritten as (Huang, 1994; Osama and Lipo, 1997)

$$\boldsymbol{C}_{\mathrm{s}}=\sqrt{\frac{2}{n}}\begin{bmatrix}\cos\varphi & \cos(\varphi-\xi) & \cos(\varphi-2\xi) & \cos(\varphi-3\xi) & \cdots & \cos[\varphi-(n-1)\xi]\\ \sin\varphi & \sin(\varphi-\xi) & \sin(\varphi-2\xi) & \sin(\varphi-3\xi) & \cdots & \sin[\varphi-(n-1)\xi]\\ \cos\varphi & \cos(\varphi-2\xi) & \cos(\varphi-4\xi) & \cos(\varphi-6\xi) & \ldots & \cos[\varphi-2(n-1)\xi]\\ \sin\varphi & \sin(\varphi-2\xi) & \sin(\varphi-4\xi) & \sin(\varphi-6\xi) & \cdots & \sin[\varphi-2(n-1)\xi]\\ \vdots & \vdots & \vdots & \vdots & \ddots & \vdots\\ \frac{1}{\sqrt{2}} & \frac{1}{\sqrt{2}} & \frac{1}{\sqrt{2}} & \frac{1}{\sqrt{2}} & \cdots & \frac{1}{\sqrt{2}}\\ \frac{1}{\sqrt{2}} & \frac{-1}{\sqrt{2}} & \frac{1}{\sqrt{2}} & \frac{-1}{\sqrt{2}} & \cdots & \frac{-1}{\sqrt{2}}\end{bmatrix}. \tag{8}$$

$$\boldsymbol{L}_{\mathrm{st}}=\begin{bmatrix}\left[L_{1\mathrm{m}}\left(1+\frac{\rho^2}{4}\right)+L_{0\mathrm{s}1}\right]\begin{bmatrix}1&0\\0&1\end{bmatrix} & \frac{\sqrt{L_{1\mathrm{m}}L_{2\mathrm{m}}}}{2g_0}\left(1-\frac{\rho^2}{4}\right)\begin{bmatrix}\alpha&-\beta\\\beta&\alpha\end{bmatrix}\\ \frac{\sqrt{L_{1\mathrm{m}}L_{2\mathrm{m}}}}{2g_0}\left(1-\frac{\rho^2}{4}\right)\begin{bmatrix}\alpha&\beta\\-\beta&\alpha\end{bmatrix} & \left[L_{2\mathrm{m}}\left(1+\frac{\rho^2}{2}\right)+L_{0\mathrm{s}2}\right]\begin{bmatrix}1&0\\0&1\end{bmatrix}\end{bmatrix}. \tag{10}$$

$$\boldsymbol{L}_{\mathrm{rt}}=\begin{bmatrix}\left[L_{1\mathrm{m}}\left(1+\frac{\rho^2}{4}\right)+L_{0\mathrm{r}1}\right]\begin{bmatrix}1&0\\0&1\end{bmatrix} & \frac{\sqrt{L_{1\mathrm{m}}L_{2\mathrm{m}}}}{2g_0}\left(1-\frac{\rho^2}{4}\right)\begin{bmatrix}\alpha&-\beta\\\beta&\alpha\end{bmatrix}\\ \frac{\sqrt{L_{1\mathrm{m}}L_{2\mathrm{m}}}}{2g_0}\left(1-\frac{\rho^2}{4}\right)\begin{bmatrix}\alpha&\beta\\-\beta&\alpha\end{bmatrix} & \left[L_{2\mathrm{m}}\left(1+\frac{\rho^2}{2}\right)+L_{0\mathrm{r}2}\right]\begin{bmatrix}1&0\\0&1\end{bmatrix}\end{bmatrix}. \tag{11}$$

$$\boldsymbol{M}_{\mathrm{srt}}=\begin{bmatrix}L_{1\mathrm{m}}\left(1+\frac{\rho^2}{4}\right)\begin{bmatrix}1&0\\0&1\end{bmatrix} & \frac{\sqrt{L_{1\mathrm{m}}L_{2\mathrm{m}}}}{2g_0}\left(1-\frac{\rho^2}{4}\right)\begin{bmatrix}\alpha&-\beta\\\beta&\alpha\end{bmatrix}\\ \frac{\sqrt{L_{1\mathrm{m}}L_{2\mathrm{m}}}}{2g_0}\left(1-\frac{\rho^2}{4}\right)\begin{bmatrix}\alpha&\beta\\-\beta&\alpha\end{bmatrix} & L_{2\mathrm{m}}\left(1+\frac{\rho^2}{2}\right)\begin{bmatrix}1&0\\0&1\end{bmatrix}\end{bmatrix}. \tag{12}$$

$$\begin{bmatrix}\boldsymbol{U}_{\mathrm{st}}\\ \boldsymbol{U}_{\mathrm{rt}}\end{bmatrix}=\begin{bmatrix}\boldsymbol{R}_{\mathrm{st}}&\boldsymbol{0}\\ \boldsymbol{0}&\boldsymbol{R}_{\mathrm{rt}}\end{bmatrix}\begin{bmatrix}\boldsymbol{I}_{\mathrm{st}}\\ \boldsymbol{I}_{\mathrm{rt}}\end{bmatrix}+\boldsymbol{L}_{\mathrm{t}}p\begin{bmatrix}\boldsymbol{I}_{\mathrm{st}}\\ \boldsymbol{I}_{\mathrm{rt}}\end{bmatrix}+\boldsymbol{G}\begin{bmatrix}\boldsymbol{I}_{\mathrm{st}}\\ \boldsymbol{I}_{\mathrm{rt}}\end{bmatrix}, \tag{14}$$

where

$$\boldsymbol{L}_{\mathrm{t}}=\begin{bmatrix}\boldsymbol{L}_{\mathrm{st}}&\boldsymbol{M}_{\mathrm{srt}}\\ \boldsymbol{M}_{\mathrm{srt}}^{\mathrm{T}}&\boldsymbol{L}_{\mathrm{rt}}\end{bmatrix},\quad \boldsymbol{U}_{\mathrm{st}}=[u_{q1\mathrm{s}}\quad u_{d1\mathrm{s}}\quad u_{q2\mathrm{s}}\quad u_{d2\mathrm{s}}]^{\mathrm{T}},\quad \boldsymbol{U}_{\mathrm{rt}}=[u_{q1\mathrm{r}}\quad u_{d1\mathrm{r}}\quad u_{q2\mathrm{r}}\quad u_{d2\mathrm{r}}]^{\mathrm{T}},$$

$$\boldsymbol{G}=\begin{bmatrix}W_{\mathrm{s}}\boldsymbol{L}_{\mathrm{st}}&W_{\mathrm{s}}\boldsymbol{M}_{\mathrm{srt}}\\ W_{\mathrm{r}}\boldsymbol{M}_{\mathrm{srt}}^{\mathrm{T}}&W_{\mathrm{r}}\boldsymbol{L}_{\mathrm{rt}}\end{bmatrix},\quad \boldsymbol{I}_{\mathrm{st}}=[i_{q1\mathrm{s}}\quad i_{d1\mathrm{s}}\quad i_{q2\mathrm{s}}\quad i_{d2\mathrm{s}}]^{\mathrm{T}},\quad \boldsymbol{I}_{\mathrm{rt}}=[i_{q1\mathrm{r}}\quad i_{d1\mathrm{r}}\quad i_{q2\mathrm{r}}\quad i_{d2\mathrm{r}}]^{\mathrm{T}},$$

$$\boldsymbol{W}_{\mathrm{s}}=\omega_1\begin{bmatrix}0&1&0&0\\-1&0&0&0\\0&0&0&1\\0&0&-1&0\end{bmatrix},$$

$$W_{\mathrm{r}}=\begin{bmatrix}0&\omega_1-\omega_{\mathrm{r}}&0&0\\-(\omega_1-\omega_{\mathrm{r}})&0&0&0\\0&0&0&\omega_1-2\omega_{\mathrm{r}}\\0&0&-(\omega_1-2\omega_{\mathrm{r}})&0\end{bmatrix}.$$

It is clearly shown that $\boldsymbol{L}_{\mathrm{st}}$, $\boldsymbol{L}_{\mathrm{rt}}$, $\boldsymbol{L}_{\mathrm{srt}}$ are all diagonal matrices when the rotor is under no eccentricity, that is, there is no mutual inductance between 1-pole-pair and 2-pole-pair equivalent windings. From Eqs.(2) and (8), it can be easily obtained that $\boldsymbol{I}_1$ and $\boldsymbol{I}_2$ are transformed to d_1-q_1 and d_2-q_2 subspaces respectively, which means that $\boldsymbol{I}_1$ and $\boldsymbol{I}_2$ are decoupled in the synchronously rotating reference frame.

Electromagnetic torque

The mechanical equation of motion is given by

$$T_{\mathrm{e}}-T_{\mathrm{r}}=J\cdot\mathrm{d}\Omega/\mathrm{d}t, \tag{15}$$

where T_{r} is the load torque, J is the mechanical motion inertia, and Ω is the speed of rotor. The motor electromagnetic torque is deduced to be

$$T_{\mathrm{e}}=2(\Psi_{d2\mathrm{m}}i_{q2\mathrm{s}}-\Psi_{q2\mathrm{m}}i_{d2\mathrm{s}})+(\Psi_{d1\mathrm{m}}i_{q1\mathrm{s}}-\Psi_{q1\mathrm{m}}i_{d1\mathrm{s}}). \tag{16}$$

ANALYTICAL MODEL OF RADIAL FORCE AND ITS VALIDATION

Radial force is crucial to the rotor suspension. The radial force acting on rotor can be calculated with virtual displacement method:

$$F_\alpha = \frac{1}{2}\begin{bmatrix} \boldsymbol{I}_{\mathrm{st}} \\ \boldsymbol{I}_{\mathrm{rt}} \end{bmatrix}^{\mathrm{T}} \frac{\mathrm{d}\boldsymbol{L}_{\mathrm{t}}}{\mathrm{d}\alpha} \begin{bmatrix} \boldsymbol{I}_{\mathrm{st}} \\ \boldsymbol{I}_{\mathrm{rt}} \end{bmatrix},\ F_\beta = \frac{1}{2}\begin{bmatrix} \boldsymbol{I}_{\mathrm{st}} \\ \boldsymbol{I}_{\mathrm{rt}} \end{bmatrix}^{\mathrm{T}} \frac{\mathrm{d}\boldsymbol{L}_{\mathrm{t}}}{\mathrm{d}\beta} \begin{bmatrix} \boldsymbol{I}_{\mathrm{st}} \\ \boldsymbol{I}_{\mathrm{rt}} \end{bmatrix}. \quad (17)$$

It is clear that the radial force is composed of two parts: one part is related to eccentricity and the other is not. The latter is used to control the rotor suspension:

$$\begin{cases} F_\alpha = \dfrac{1}{2g_0\sqrt{L_{1\mathrm{m}}L_{2\mathrm{m}}}}(\Psi_{d2\mathrm{m}}\Psi_{d1\mathrm{m}} + \Psi_{q2\mathrm{m}}\Psi_{q1\mathrm{m}}), \\ F_\beta = \dfrac{1}{2g_0\sqrt{L_{1\mathrm{m}}L_{2\mathrm{m}}}}(\Psi_{q2\mathrm{m}}\Psi_{d1\mathrm{m}} - \Psi_{d2\mathrm{m}}\Psi_{q1\mathrm{m}}), \end{cases} \quad (18)$$

where

$$\Psi_{d1\mathrm{m}} = L_{1\mathrm{m}}(i_{d1\mathrm{s}} + i_{d1\mathrm{r}}),\ \Psi_{q1\mathrm{m}} = L_{1\mathrm{m}}(i_{q1\mathrm{s}} + i_{q1\mathrm{r}}),$$
$$\Psi_{d2\mathrm{m}} = L_{2\mathrm{m}}(i_{d2\mathrm{s}} + i_{d2\mathrm{r}}),\ \Psi_{q2\mathrm{m}} = L_{2\mathrm{m}}(i_{q2\mathrm{s}} + i_{q2\mathrm{r}}).$$

The radial force and the rotor displacement in stationary reference frame are given by

$$\begin{bmatrix} \ddot{\alpha} \\ \ddot{\beta} \end{bmatrix} = \frac{1}{m}\begin{bmatrix} F_\alpha \\ F_\beta - G_{\mathrm{r}} \end{bmatrix}, \quad (19)$$

where m and G_{r} are the mass and weight of rotor respectively.

The analytical model of radial force is verified using FEA software ANSOFT. The FE model is the 5-phase motor as shown in Fig.1. The parameters are chosen as follows: turns per phase: 120; stack length: l=90 mm; air-gap thickness: g_0=0.55 mm; radius of air gap: r=57.7 mm. The inductances are calculated by Maxwell2D. The comparisons between analytical results of radial force and FEA results are shown in Figs.5 and 6.

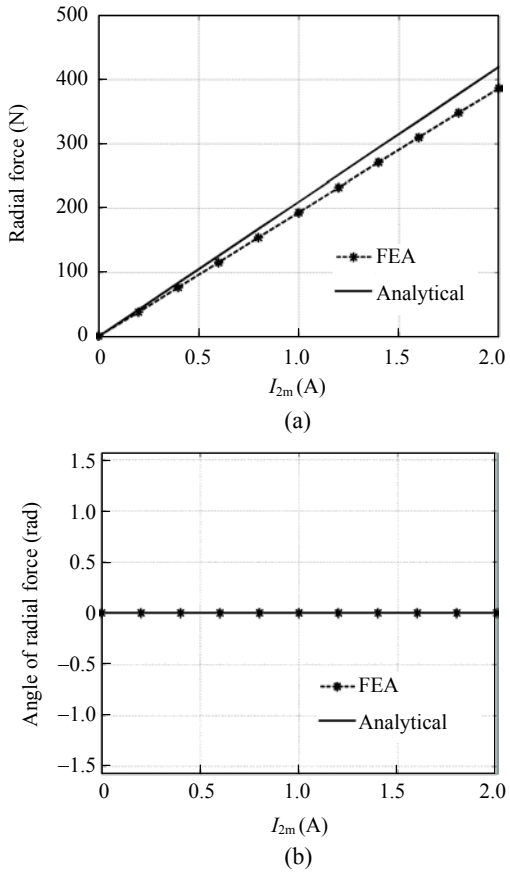

Fig.5 Radial force vs $I_{2\mathrm{m}}$ with $I_{1\mathrm{m}}$=1 A, Φ_1=0, Φ_2=0. (a) Radial force; (b) Angle of radial force

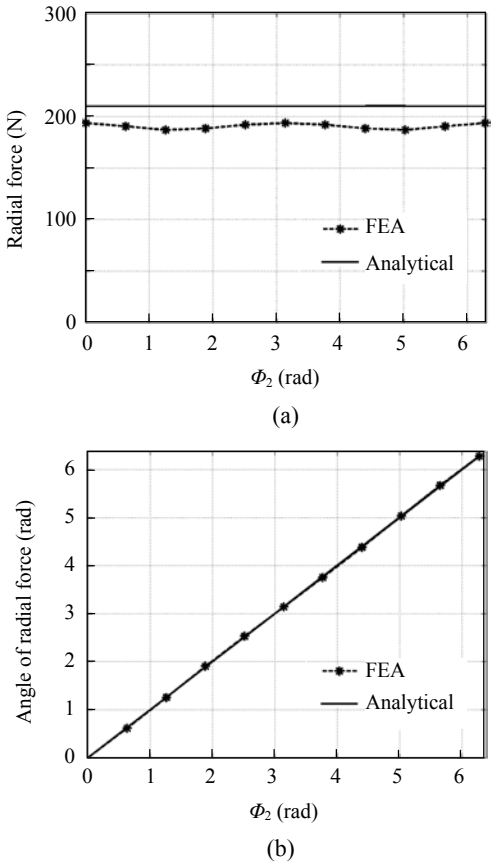

Fig.6 Radial force vs Φ_2 with $I_{1\mathrm{m}}$=1 A, $I_{2\mathrm{m}}$=1 A, Φ_1=0. (a) Radial force; (b) Angle of radial force

Fig.5 shows that the magnitude of radial force is proportional to the increasing current $\boldsymbol{I}_2$ for a fixed $\boldsymbol{I}_1$, and that the angle of radial force is constant when Φ_1 and Φ_2 are fixed. The angle of radial force is zero when the force has the same direction as the axis of phase "*a*".

As shown in Fig.6, the magnitude of radial force is invariable when I_{1m} and I_{2m} are constant, while the angle of radial force varies with Φ_1.

Analytical results and FEA results are plotted by solid line and dashed line respectively. It is clear that the analytical results are in close agreement with FEA results, so this analytical model can well describe the characteristics of radial force.

CONTROL AND SIMULATION OF BEARINGLESS MOTOR WITH MULTIPHASE WINDINGS

Taking a 5-phase induction motor as example, "5-phase 1-pole-pair currents" $\boldsymbol{I}_1$ (namely i_{q1s}, i_{d1s}) can be seen as the "motor currents", and "5-phase 2-pole-pair currents" $\boldsymbol{I}_2$ (namely i_{q2s}, i_{d2s}) are the "levitation currents". The "motor currents" equations under no eccentricity are rewritten as

$$\begin{bmatrix} u_{q1s} & u_{d1s} & 0 & 0 \end{bmatrix}^{\mathrm{T}} = \begin{bmatrix} R_{1s}+pL_{1s} & \omega_1 L_{1s} & pL_{1m} & \omega_1 L_{1m} \\ \omega_1 L_{1s} & R_{1s}+pL_{1s} & \omega_1 L_{1m} & pL_{1m} \\ pL_{1m} & (\omega_1-\omega_r)L_{1m} & R_{1r}+pL_{1r} & (\omega_1-\omega_r)L_{1r} \\ (\omega_1-\omega_r)L_{1m} & pL_{1m} & (\omega_1-\omega_r)L_{1r} & R_{1r}+pL_{1r} \end{bmatrix} \cdot \begin{bmatrix} i_{q1s} & i_{d1s} & i_{q1r} & i_{d1r} \end{bmatrix}^{\mathrm{T}}. \tag{20}$$

In the air-gap-flux-oriented control system, one can easily obtain

$$\Psi_{d1m}=\Psi_{1m},\ \Psi_{q1m}=0, \tag{21}$$

Substituting Eq.(21) into Eq.(20) yields

$$i_{d1s}=[(R_{1r}+pL_{1r})\Psi_{1m}/L_{1m}+(\omega_1-\omega_r)L_{01r}i_{q1s}] \cdot (R_{1r}+pL_{01r})^{-1}, \tag{22}$$

$$\omega_s=\omega_1-\omega_r=\frac{(R_{1r}+pL_{01r})i_{q1s}}{L_{1r}\Psi_{1m}/L_{1m}-L_{01r}i_{d1s}}. \tag{23}$$

"Levitation currents" generate 2-pole-pair magnetic field which rotates at $\omega_1/2$, that is, "levitation currents" generate a very small negative torque. Therefore,

$$T_e\approx\Psi_{d1m}i_{q1s}-\Psi_{q1m}i_{d1s}=\Psi_{1m}i_{q1s}, \tag{24}$$

$$i_{q1s}=T_e/\Psi_{1m}, \tag{25}$$

$$\begin{bmatrix} F_\alpha \\ F_\beta \end{bmatrix}=\frac{L_{2m}}{2g_0\sqrt{L_{1m}L_{2m}}}\Psi_{1m}\begin{bmatrix} i_{d2m} \\ i_{q2m} \end{bmatrix}, \tag{26}$$

where $i_{d2m}=i_{d2s}+i_{d2r}$, $i_{q2m}=i_{q2s}+i_{q2r}$.

Fig.7 shows the block diagram of air-gap-flux-oriented control system configuration of a 5-phase bearingless motor. The control strategy is very similar to the control system of conventional bearingless motors (Chiba *et al*., 1997; Suzuki *et al*., 2000). The "motor currents" command i_{q1s}^*, i_{d1s}^* are generated from air-gap-flux-oriented control, and "levitation currents" command i_{q2s}^*, i_{d2s}^* are generated by compensating i_{q2m}^*, i_{d2m}^* for the influence of i_{q2r}^* and i_{d2r}^* (Nomura *et al*., 1993). i_{q2m}^* and i_{d2m}^* are obtained by Eq.(26). Phase currents are given by the 5-phase inverse transformation of i_{q1s}^*, i_{d1s}^* and i_{q2s}^*, i_{d2s}^*.

The motor parameters are: L_{1m}=0.247 H, L_{2m}=0.046 H, L_{0s1}=L_{0r1}=0.0045 H, L_{0s2}=L_{0r2}=0.0040 H; R_{1s}=R_{2s}=1.2 Ω; R_{1r}=0.47 Ω; R_{2r}=0.27 Ω; m=10 kg, J=0.01 kg·m^2, length of air gap g_0=0.55 mm, and the air-gap length between the rotor shaft and the touchdown bearing is 0.3 mm. Simulation results are shown in Figs.8 and 9.

Fig.8 presents the speed and rotor displacement during the start up. It is clear that the shaft is successfully suspended and that the rotor suspension is stable with radial displacement variations of less than 50 μm. Fig.9 shows the stator currents. The amplitudes of i_a and i_b are unequal because two groups of currents ($\boldsymbol{I}_1$ and $\boldsymbol{I}_2$) are fed. Therefore, the proposed bearingless motor with a single set of multiphase windings is feasible. The experimental results will be presented in future work.

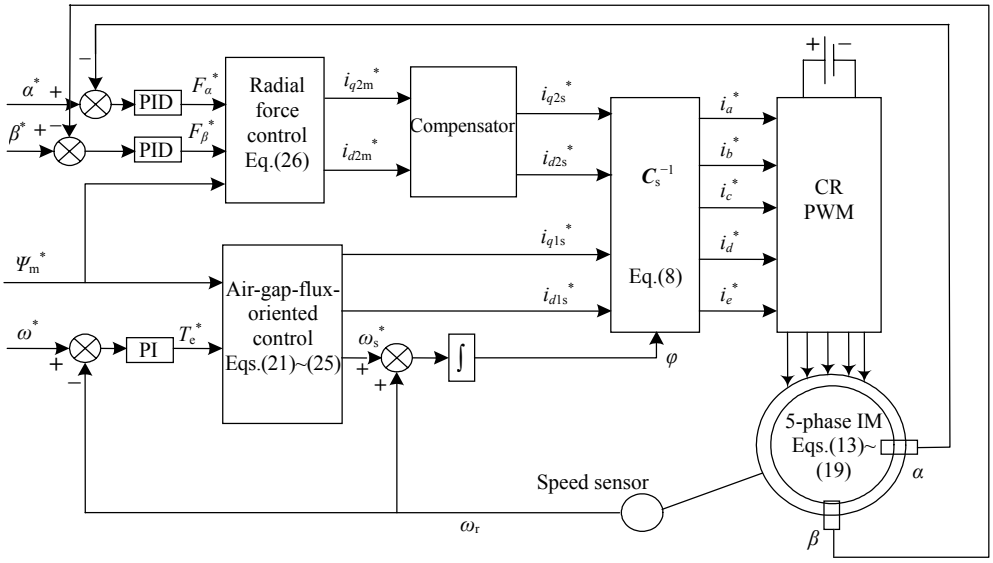

Fig.7 Air-gap-flux-oriented control diagram of a 5-phase bearingless motor

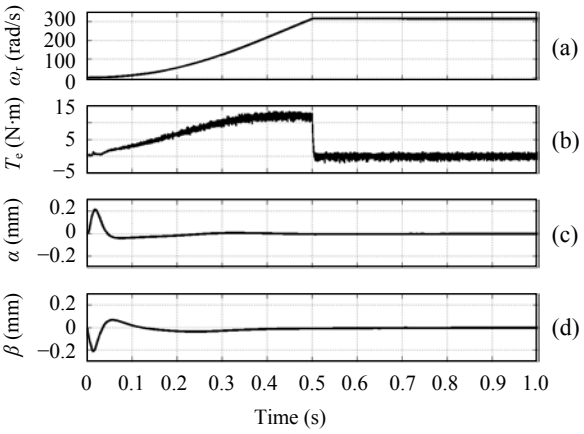

Fig.8 Simulation results of the air-gap-flux-oriented control system of a 5-phase bearingless induction motor. (a) Rotor speed ω_r; (b) Torque T_e; (c) Rotor displacement α; (d) Rotor displacement β

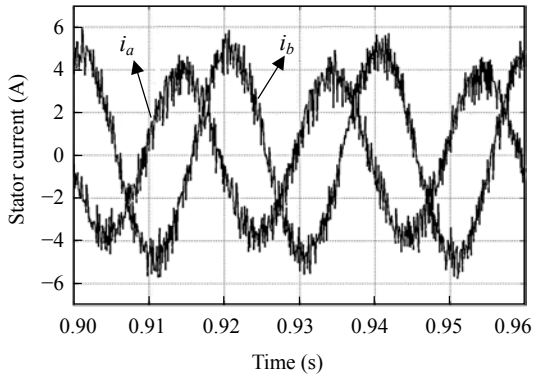

Fig.9 Simulation results of the stator phase currents

CONCLUSION

This paper sets forth a bearingless motor with a single set of multiphase windings (phase number $n \geq 5$). The model is proposed based on the principles of radial force generation and multiphase theory. Its torque and rotor suspension are realized by feeding two groups of currents to the single set of multiphase windings. The inductance matrices under eccentricity are deduced with modified winding function method, based on which the mathematical model of this new bearingless motor is also developed. Air-gap-flux-oriented control system is designed and simulation results verified the feasibility of this bearingless motor.

The proposed motor not only possesses advantages of bearingless motors with a single set of windings (i.e. simpler construction, less switches and relatively low power loss) but also possesses advantages of multiphase machines (i.e. achieving high power ratings with lower voltage limited devices). This method is also applicable to other bearingless motors such as permanent magnet motors and reluctance motors.

References

Chiba, A., Deido, T., Fukao, T., Rahman, M.A., 1994. An analysis of bearingless AC motors. *IEEE Trans. on Energy Conv.*, **9**(1):61-68. [doi:10.1109/60.282477]

Chiba, A., Furuichi, R., Aikawa, Y., Shimada, K., Takamoto, Y., Fukao, T., 1997. Stable operation of induction-type

bearingless motors under loaded conditions. *IEEE Trans. on Ind. Appl.*, **33**(4):919-924. [doi:10.1109/28.605733]

Faiz, J., Tabatabaei, I., 2002. Extension of winding function theory for nonuniform air gap in electric machinery. *IEEE Trans. on Magn.*, **38**(6):3654-3657. [doi:10.1109/TMAG.2002.804805]

Ferreira, J.M.S., Zucca, M., Salazar, A.O., Donadio, L., 2005. Analysis of bearingless machine with divided windings. *IEEE Trans. on Magn.*, **41**(10):3931-3933. [doi:10.1109/TMAG.2005.854972]

Huang, J., 1994. Application of *p*-pair poles *n*-phase transformation in the analysis of synchronous machines with stator winding fault. *Proc. CSEE*, **14**(5):10-17 (in Chinese).

Khoo, S.W.K., 2005. Bridge configured winding for polyphase self-bearing machines. *IEEE Trans. on Magn.*, **41**(4):1289-1295. [doi:10.1109/TMAG.2005.845837]

Levi, E., Jones, M., Vukosavic, S.N., Toliyat, H.A., 2004. A novel concept of a multiphase, multimotor vector controlled drive system supplied from a single voltage source inverter. *IEEE Trans. on Power Electr.*, **19**(2):320-335. [doi:10.1109/TPEL.2003.823241]

Luo, X.G., Liao, Y.F., Toliyat, H.A., EI-Anatbly, A., Lipo, T.A., 1995. Multiple coupled circuit modeling of induction machines. *IEEE Trans. on Ind. Appl.*, **31**(2):311-318. [doi:10.1109/28.370279]

Nomura, S., Chiba, A., Nakamura, F., Ikeda, K., Fukao, T., Rahman, M.A., 1993. A Radial Position Control of Induction Type Bearingless Motor Considering Phase Delay Caused by the Rotor Squirrel Cage. IEEE Power Conversion Conference. Yokohama, Japan, p.438-443. [doi:10.1109/PCCON.1993.264144]

Okada, Y., Dejima, K., Ohishi, T., 1995. Analysis and comparison of PM synchronous motor and induction motor type magnetic bearing. *IEEE Trans. on Ind. Appl.*, **31**(5):1047-1053. [doi:10.1109/28.464518]

Osama, M., Lipo, T.A., 1997. Modeling and analysis of a wide speed-range induction motor drive based on electronic pole changing. *IEEE Trans. on Ind. Appl.*, **33**(5):1177-1184. [doi:10.1109/28.633794]

Osama, M., Lipo, T.A., 1999. A Magnetic Relief Scheme for Four Pole Induction Motors. Conference on Electrical Machines, Converters and Systems. Lisbon, Portugal, p.I15-I21.

Suzuki, T., Chiba, A., Rahman, M.A., Fukao, T., 2000. An air-gap flux-oriented vector controller for stable operation of bearingless induction motors. *IEEE Trans. on Ind. Appl.*, **36**(4):1069-1076. [doi:10.1109/28.855962]

Xu, H., Toliyat, H.A., Petersen, L.J., 2001. Rotor Field Oriented Control of a Five-Phase Induction Motor with the Combined Fundamental and Third Harmonic Currents. Applied Power Electronics Conference and Exposition, p.392-398.